DOI: 10.1534/genetics.104.039735

# *RacGap50C* Negatively Regulates Wingless Pathway Activity During Drosophila Embryonic Development

**Whitney M. Jones and Amy Bejsovec**[1]

*Department of Biology, Duke University, Durham, North Carolina 27708-1000*

Manuscript received December 14, 2004
Accepted for publication January 3, 2005

ABSTRACT

The Wingless (Wg)/Wnt signal transduction pathway directs a variety of cell fate decisions in developing animal embryos. Despite the identification of many Wg pathway components to date, it is still not clear how these elements work together to generate cellular identities. In the ventral epidermis of Drosophila embryos, Wg specifies cells to secrete a characteristic pattern of denticles and naked cuticle that decorate the larval cuticle at the end of embryonic development. We have used the Drosophila ventral epidermis as our assay system in a series of genetic screens to identify new components involved in Wg signaling. Two mutant lines that modify *wg*-mediated epidermal patterning represent the first loss-of-function mutations in the *RacGap50C* gene. These mutations on their own cause increased stabilization of Armadillo and cuticle pattern disruptions that include replacement of ventral denticles with naked cuticle, which suggests that the mutant embryos suffer from ectopic Wg pathway activation. In addition, *RacGap50C* mutations interact genetically with *naked cuticle* and *Axin*, known negative regulators of the Wg pathway. These phenotypes suggest that the *RacGap50C* gene product participates in the negative regulation of Wg pathway activity.



THE Wnt signaling pathway plays a critical role in many developmental processes. Of the 19 mouse *Wnt* genes, 10 have been characterized mutationally and each directs patterning and cell fate decisions in a different tissue, such as brain, somites, kidneys, and limbs (reviewed in Wodarz and Nusse 1998; Logan and Nusse 2004). In Drosophila, a single Wnt molecule, encoded by the *wingless* (*wg*) gene, alone directs a similar range of cell fate and patterning decisions, specifying cell fate in the central nervous system, larval muscle, Malpighian tubules, and appendages (reviewed in Dierick and Bejsovec 1999). Although other *Wnt* genes are present in the fly genome, they do not appear to have major roles in development (reviewed in Logan and Nusse 2004).

Wg signaling is most easily assayed in the embryonic epidermis. Epidermal cells are exquisitely sensitive to Wg signaling levels and so this tissue provides a useful model to investigate the proteins involved in the pathway and to explore how they work together to generate pattern. Ventral epidermal cells secrete a segmentally repeating pattern of small hooks, called denticles, separated by expanses of naked cuticle (Lohs-Schardin *et al.* 1979; Wieschaus and Nüsslein-Volhard 1986). These belts of denticles provide traction for the crawling larva after it hatches from the egg. In abdominal segments 2–7, each belt contains six rows of denticles. Each row of denticles shows a characteristic morphology that requires input from Wg signaling in the epidermal cells prior to stage 10 or ~6 hr after egg laying (Bejsovec and Martinez-Arias 1991; Moline *et al.* 1999). Wg signaling at later stages specifies the expanses of naked cuticle that separate the denticle belts (Bejsovec and Martinez-Arias 1991). Loss-of-function *wg* mutations alter the cuticle pattern profoundly: mutant embryos secrete no naked cuticle and instead produce a continuous lawn of denticles, all with a similar morphology (Nüsslein-Volhard *et al.* 1984; Bejsovec and Wieschaus 1993). Conversely, ectopic overexpression of *wg* redirects all of the epidermal cells into the naked cuticle cell fate, resulting in a uniform expanse of smooth cuticle (Noordermeer *et al.* 1992).

Wg protein specifies cell fates by activating an intracellular signaling cascade, the components of which are highly conserved among animal species (reviewed in Cadigan and Nusse 1997; Wodarz and Nusse 1998; Dierick and Bejsovec 1999). The activity of the pathway hinges on regulation of Armadillo (Arm), the fly homolog of β-catenin. In the absence of Wg signal, Arm is present at adherens junctions, but is kept at low levels in the cytoplasm. This downregulation is accomplished by a set of proteins collectively known as the destruction complex, which includes Axin, Apc2, and the kinase Zeste-white 3 (Zw3). The complex phosphorylates Arm, targeting it for destruction by the proteasome (reviewed in Peifer and Polakis 2000; Jones and Bejsovec 2003). When Wg binds to its receptor, Dfz2, and coreceptor, Arrow, the clustering of the cell surface molecules somehow activates Dishevelled (Dsh) and leads to the degradation of Axin (Tolwinski *et al.* 2003). Degradation of

[1]*Corresponding author:* Department of Biology, Duke University, DCMB Group/Box 91000, B336 LSRC, Research Dr., Durham, NC 27708-1000. E-mail: bejsovec@duke.edu

Axin and disruption of the destruction complex allows Arm to accumulate in the cytoplasm and in the nucleus. In the nucleus, Arm binds to the DNA-binding protein Tcf (also known as Pangolin or LEF) and activates downstream gene transcription (Brunner *et al.* 1997; van de Wetering *et al.* 1997). Depending on the tissue and the time of development, different downstream genes are activated.

The Wg pathway components characterized to date were identified primarily through their mutant phenotypes in Drosophila. Loss of a pathway activator mimics the phenotype of *wg* null mutants, resulting in embryos that secrete a uniform lawn of denticles. Loss of a negative regulatory component mimics the effect of ectopic *wg* overexpression, producing a uniform naked cuticle phenotype. Despite the many components implicated in pathway modulation, their interactions and precise mechanisms of action are still somewhat mysterious. For example, it is not clear how Dsh, the most upstream cytosolic component in the Wg pathway, interacts with the receptor complex to mediate inactivation of the destruction complex. Our laboratory has sought to fill the gaps by isolating mutations that modify Wg pathway activity. Here we describe loss-of-function mutations in one such component, encoded by the *RacGap50C* locus, which were isolated through their suppression of a hypomorphic *wg* mutant allele.

## MATERIALS AND METHODS

**Drosophila stocks and culture conditions:** All deficiencies and *P*-element insertions were obtained from the Bloomington Stock Center. *P{UAS-DRacGap$^{+}$}* and *P{UAS-DRacGap$^{\Delta EIE}$}*, a dominant-negative form of *RacGap50C* with GAP domain amino acids 405–407 deleted, were kindly provided by S. Campuzano (Sotillos and Campuzano 2000). The *P{UAS-nkd}* transgenes (Zeng *et al.* 2000) were a gift from K. Wharton and M. Scott. *P{UAS-Rac1.V12}* and *P{UAS-Rac1.N17}*, the constitutively active and dominant-negative forms of *Rac1*, respectively (Luo *et al.* 1994), and *P{UAS-AxinGFP}* (Cliffe *et al.* 2003) were obtained from the Bloomington Stock Center. Ubiquitous embryonic expression of *UAS* transgenes was achieved with either the *E22C-Gal4* or the *arm-Gal4* driver lines. Both were tested in each assay and produced similar results unless otherwise noted. More restricted embryonic expression was achieved using the *prd-Gal4* and *wg-Gal4* driver lines. All driver lines are available from the Bloomington Stock Center.

The *naked cuticle* (*nkd*) allele used in this study, *nkd$^{7E89}$*, is a strong hypomorph (Jürgens *et al.* 1984; Zeng *et al.* 2000). The *AR2* and *DH15* mutations were induced on a *wg$^{IL114}$* chromosome, as described below, and were subsequently recombined away from *wg* for further analysis. The mutant chromosomes were extensively recombined with wild type (Oregon-R) to remove unrelated lethal mutations and were rebalanced over a *CyO* chromosome carrying *Kruppel-Gal4 UAS-GFP* inserts (obtained from Bloomington) to allow identification of homozygous-mutant embryos by their failure to fluoresce.

Flies were reared on cornmeal-agar-molasses unless otherwise noted. For analysis of embryonic stages, eggs were collected on apple juice-agar plates and aged at 25°. To examine embryonic cuticles, eggs were allowed to develop fully (24 hr at 25°), dechorionated in bleach, and transferred to a drop of Hoyer's medium, mixed 1:1 with lactic acid (Wieschaus and Nüsslein-Volhard 1986), on a microscope slide. Mechanical devitellinization was performed by exerting gentle pressure on the coverslip to burst the vitelline membrane. Cuticle preparations were baked at 65° overnight before viewing on a Zeiss Axioplan microscope with phase optics.

**Isolation and characterization of mutant alleles:** The *AR2* and *DH15* mutant lines were isolated independently in a genetic screen for modifiers of the *wg* mutant phenotype. The temperature-sensitive *wg* allele, *wg$^{IL114}$*, used in this screen is also known as *wg$^{ts}$* or *wg$^{l\text{-}12}$*. Male *wg$^{IL114}$/CyO* flies were fed overnight on ethyl methanesulfonate (EMS) at a concentration of 25 mm in 1% sucrose. They were allowed to recover and mated with virgin *Dominant temperature sensitive (DTS)/CyO* females (Nüsslein-Volhard *et al.* 1984). At 29°, only flies bearing the mutagenized *wg$^{IL114}$* chromosome over *CyO* survive, and these were mated singly with *DTS/CyO* flies and raised at 29° to establish isogenic lines. A total of 1768 lines were established, and their $F_3$ progeny were examined for alteration of the *wg$^{IL114}$* cuticle pattern at 25°.

The *AR2* and *DH15* mutations were tested for complementation because they yielded similar modifications of the *wg$^{IL114}$* pattern. They failed to complement each other in this modification, and when recombined away from the linked *wg$^{IL114}$* mutation, their homozygous-recessive embryonic-lethal phenotypes also failed to complement. The mutations were mapped using meiotic recombination against a second chromosome marked with the adult visible mutations *black*, *purple*, *cinnabar*, *curved*, *plexus*, and *speck*. The mutations mapped between *cinnabar* and *curved* at ~70 MU, and deficiencies in this region were tested for their failure to complement. Both alleles failed to complement *Df(2R)CX1*, which removes cytological position 49C1-4;50C23-D2, and to complement *Df(2R)vgB*, which removes 49D3-4;49F15-50A3. We mapped *AR2* and *DH15* more precisely using site-specific *P*-element-mediated recombination in males (Chen *et al.* 1998). The *P* elements used for mapping the two alleles include *P{lacW}drk$^{k02401}$*, *P{PZ}drk$^{10626}$*, *P{EP}EP2007*, *P{PZ}fas$^{05488}$*, *P{lacW}v(2)k16105$^{k16105}$*, *P{EP}EP2423*, *P{lacW}shot$^{k03010}$*, *P{lacW}AGO1$^{k08121}$*, *P{lacW}AGO1$^{k00208}$*, *P{PZ}AGO1$^{04845}$*, and *P{lacW}Cp1$^{k15606}$*.

The mutations mapped between *P{EP}EP2423* and *P{lacW}shot$^{k03010}$*, narrowing down the interval to 13 annotated open reading frames, 6 of which were predicted to encode "housekeeping" enzymes. The complete sequences of all exons from the 7 other candidate genes in the *AR2* and *DH15* mutant lines were compared to the consensus sequence to locate the EMS-induced mutations. PCR primers were designed using MacVector software and tested using Amplify (W. R. Engels). PCR was performed with both homozygous and heterozygous genomic DNA. The products were purified using the QIAquick PCR purification kit (QIAGEN, Chatsworth, CA) and sequenced using ABI PRISM dye terminator cycle sequencing ready reaction kit with Amplitaq DNA polymerase according to manufacturer's protocols. Both alleles were found to encode nonsense mutations in the *RacGAP50C* gene, CG13345. The PCR primers used to identify the single nucleotide changes in the *RacGAP50C* gene include 5′-CGAGTGAAAACCGATTCGTAG-3′, 5′-AGGTGTGGTTCCTCATCAG-3′, 5′-GGTAAATGCTATGGCACCTC-3′, and 5′-CGTCAAATGCTTTCCAACAAGG-3′. Additional primers used for sequencing *DRacGAP50C* were 5′-ATCTGAACAACGAGACCC-3′, 5′-GGTATCTGCTCACCGTTAGC-3′, and 5′-TCCTGGGAGTTTTGGTGTC-3′.

**Antibody staining and *in situ* hybridization:** RNA *in situ* hybridization was performed with antisense digoxigenin-labeled probes following standard protocols (Ashburner 1989; Tautz and Pfeifle 1989). Antibody staining was as described in Dierick and Bejsovec (1998). Anti-Wg antibody was used

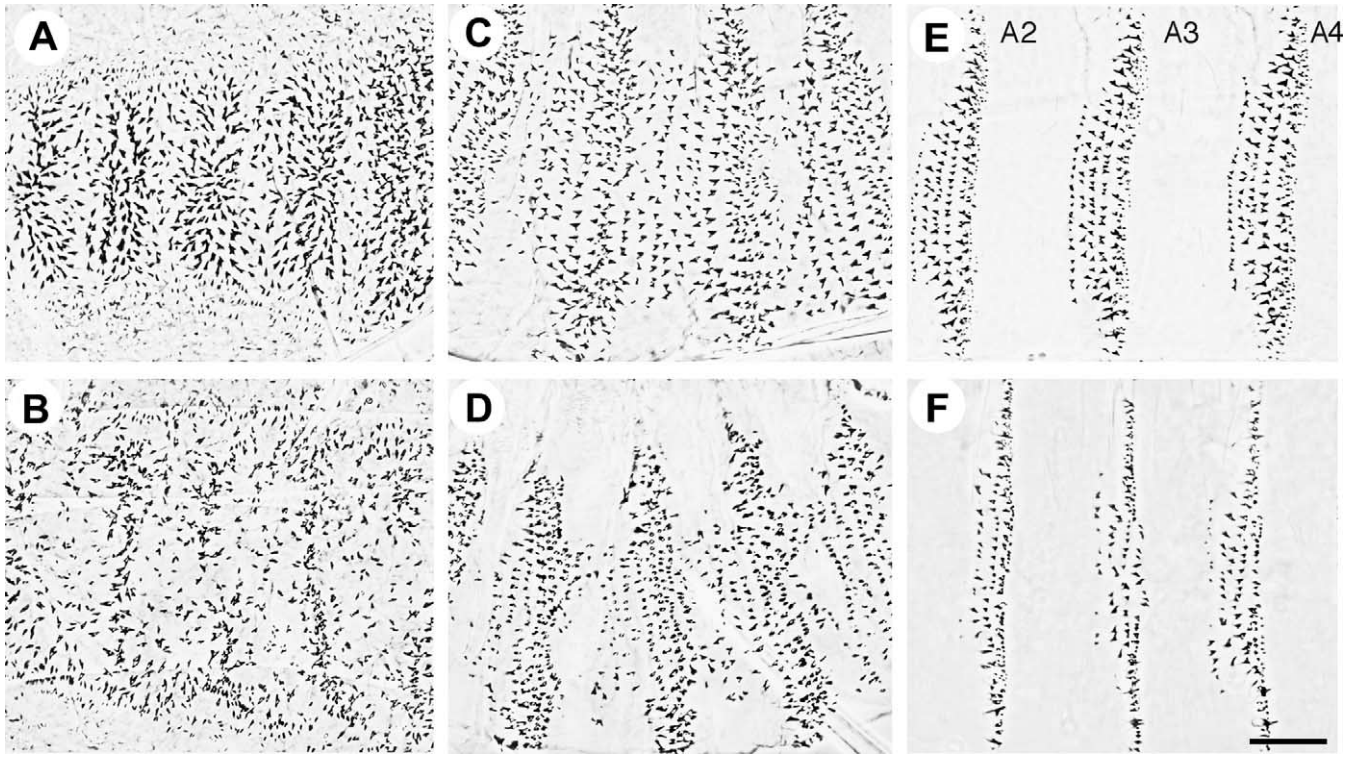


FIGURE 1.—Epidermal patterning is altered in *AR2* and *DH15* homozygous-mutant embryos. (A) The $wg^{IL114}$ allele at the restrictive temperature produces the "lawn of denticles" phenotype characteristic of *wg* loss-of-function mutations. (B) This severe patterning defect is altered in $wg^{IL114}$ *AR2* doubly mutant embryos, which are larger than the *wg* single-mutant embryo. (C) The $wg^{PE2}$ hypomorphic allele produces a weaker pattern defect, with normal segmental patterning of the denticle rows but loss of the intervening naked cuticle expanse. (D) Some naked cuticle is restored in $wg^{PE2}$ *AR2* double-mutant embryos, indicating that the weak Wg signaling promoted by $wg^{PE2}$ mutant protein is enhanced. (E) Wild-type embryos secrete a stereotyped pattern of six rows of denticles interspersed with naked cuticle in each abdominal segment. Abdominal segments 2–4 are shown. (F) In each abdominal segment, some denticle rows are replaced by naked cuticle in embryos homozygous for the *AR2* mutation. In this and all subsequent figures, anterior of the embryo is to the left. Bar, 100 μm.

at 1:1000 and anti-Arm was used at 1:50 (both from the Developmental Studies Hybridoma Bank). Anti-Coracle antibody (kindly provided by R. Fehon) was used at 1:10,000. DAPI stain was used at 1:20,000. Cy3 and Cy5 IgG secondary antibodies (Jackson ImmunoResearch, West Grove, PA) were used to detect fluorescence staining. Embryos were mounted in Aquapolymount (Polysciences, Niles, IL) and viewed with a Zeiss 410 confocal microscope.

**Hatching efficiencies and cuticle pattern analysis:** Fly crosses were performed at 25°, and eggs were collected in 2- to 4-hr time windows. Eggs were arrayed on apple juice agar plates and counted before being allowed to age for 24 hr at 25°. Unhatched eggs were then dechorionated with bleach and mounted in Hoyer's medium for scoring; in some cases hatched larvae were mounted as well. The number of unfertilized eggs was subtracted from the total egg count, prior to calculating proportions for different phenotypic classes. Denticle rows in abdominal segments 3–6 were examined in at least 20 embryos for each genotype, concentrating on the middle one-third of the belt centered over the ventral midline.

**Immunoblot analysis:** Five- to 7-hr-old embryos were collected, dechorionated, and examined for the presence or absence of GFP from the *Kr-GFP CyO* balancer. Fifteen homozygous-mutant embryos (identified by lack of fluorescence) as well as 15 wild-type siblings (identified by twofold brightness of fluorescence) were collected and immunoblots were performed as described in CHAO *et al.* (2003). Filters were stained with anti-Arm protein (Developmental Studies Hybridoma Bank) at 1:100 and with antitubulin at 1:5000 (Labvision). Cross-reacting proteins were detected and quantified using the Odyssey infrared imaging system and reagents (Li-Cor Technologies).

## RESULTS

***AR2* and *DH15* modify *wg* phenotypes:** In a genetic screen to identify mutations that suppress or enhance the mutant phenotype of the *wg* temperature-sensitive allele $wg^{IL114}$, we isolated two EMS-induced mutations that subtly modify the $wg^{IL114}$ mutant cuticle pattern. These modifier mutations, *AR2* and *DH15*, fail to complement each other and thus identify a single complementation group, linked to *wg* on the second chromosome. These two alleles produce identical phenotypes in our assays: all figures shown use the *AR2* line; however, similar results were obtained using *DH15*. Both mutations show no increase in severity when placed in *trans* to a deficiency for the region and so are likely to represent loss-of-function alleles.

$wg^{IL114}$ embryos at the restrictive temperature are much smaller than wild-type embryos and secrete the "lawn of denticles" cuticle pattern typical of low pathway

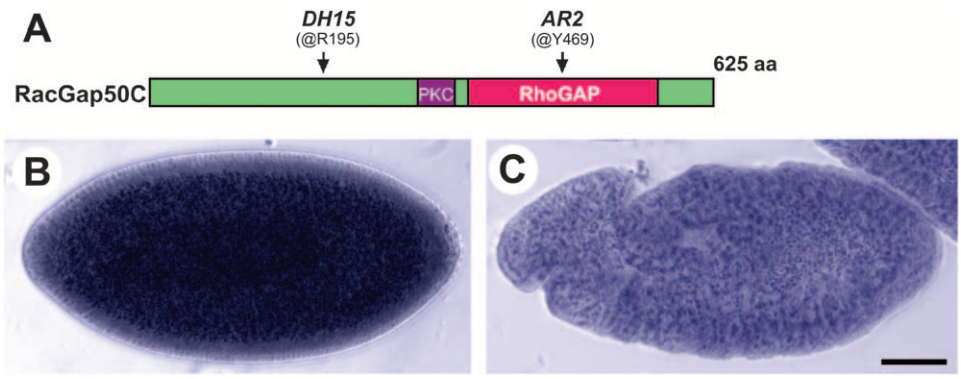


FIGURE 2.—*RacGap50C* is mutated in *AR2* and *DH15*. (A) Structure of *RacGap50C* predicted protein, with position of premature termination codons noted and positions of the PKC and GTPase-activating domain homologies highlighted. Overall, the predicted RacGap50C protein is 32% identical to the human RacGap1, and in the GAP region, the identity is 51% (using Clustal alignment). In the Drosophila genome, RacGap50C is most closely related to RacGap84C (24% identical, 56% in the GAP region) but shares homology in the GAP region with other members of the Rho family GTPase-activating proteins. (B) *RacGap50C* mRNA appears to be loaded into the egg maternally since early stage wild-type embryos, such as the stage 4 embryo shown here, stain heavily in RNA *in situ* hybridizations. (C) Stage 10 embryo shows the uniform low level of *RacGap50C* mRNA detected at later stages of wild-type embryonic development. Bar, 100 μm.

activity (Figure 1A). The modifier lines *AR2* and *DH15* were found to alter the $wg^{IL114}$ phenotype in a similar way, increasing the spacing between denticles and the overall body size of the doubly mutant embryos (Figure 1B). This phenotype indicates that the modifier mutations considerably reduce the severity of the *wg* loss-of-function phenotype, resulting in a larger, healthier embryo even though the cuticle pattern is only subtly altered. Both *AR2* and *DH15* also modify other *wg* alleles, including $wg^{CX4}$, an RNA null allele of *wg* (not shown). The cuticle pattern defects of weak *wg* alleles are more dramatically suppressed by the *AR2* and *DH15* mutations. The $wg^{PE2}$ hypomorphic allele produces a protein with a lower affinity for the receptor complex (BEJSOVEC and WIESCHAUS 1995; MOLINE *et al.* 2000). $wg^{PE2}$ homozygous mutants show segmental denticle diversity, but little or no naked cuticle separating the belts (Figure 1C). The $wg^{PE2}$ *AR2* doubly homozygous mutants show an increase in the amount of naked cuticle, indicating that some Wg signaling is restored (Figure 1D).

In an otherwise wild-type background, the *AR2* and *DH15* mutations are recessive lethal, and homozygous embryos show an excess specification of naked cuticle at the expense of denticles. Wild-type embryos (Figure 1E) secrete an average of 5.95 ± 0.15 rows of denticles/belt ($n = 40$) in abdominal segments 3–6. In contrast, *AR2* mutant embryos secrete an average of only 3.95 ± 0.64 rows of denticles/belt ($n = 80$) (Figure 1F). The mutant denticles also differ morphologically from the wild type. Wild-type denticles show a wide range in size, with those in row 5 being largest (BEJSOVEC and WIESCHAUS 1993). The *AR2* and *DH15* mutant denticle belts contain fewer of these large denticles: most denticles observed are similar in size to the smaller denticles normally found in rows 1–4 of the wild-type belt pattern. The slight suppression of *wg* mutant phenotypes and the ectopic specification of naked cuticle are consistent with an increase in Wg pathway activity, suggesting that the *AR2* and *DH15* mutations might disrupt a negative regulator of the pathway.

***AR2* and *DH15* carry nonsense mutations disrupting the *RacGap50C* locus:** The *AR2* and *DH15* mutations were mapped on the second chromosome, using standard meiotic recombination and deficiency analysis. Male site-specific recombination further refined the interval to cytological region 50C06-09. Seven candidate genes within this interval were sequenced and lesions in only the *RacGap50C* locus were detected for both the *AR2* and *DH15* lines. *RacGap50C* encodes one of two RacGaps annotated in the Drosophila genome (ADAMS *et al.* 2000; FlyBase at http://flybase.bio.indiana.edu/). While the genome contains 21 predicted Rho family GTPase-activating proteins (BERNARDS 2003), only *RacGap50C* and *RacGap84C* are strongly conserved with the human RacGap1. The predicted RacGap50C polypeptide contains a protein kinase C (PKC) conserved region, which is predicted to bind diacylglycerol, as well as a RhoGap motif, a 140-amino-acid GTPase-activating domain that stimulates the Rho-like GTPases, Rac, Rho, or Cdc42 (Figure 2A). *AR2* carries a point mutation in the *RacGap50C* coding region that changes amino acid 470, a tryptophan, to a premature stop. This is predicted to truncate the protein within the RhoGap domain. *DH15* encodes a mutation at amino acid 195, changing an arginine to a stop and truncating the protein prior to both the PKC domain and the RhoGap domain.

Previous work using misexpression constructs indicated that *RacGap50C* modulates EGF pathway activity in the developing wing (SOTILLOS and CAMPUZANO 2000) and plays a critical role in cytokinesis (SOMERS and SAINT 2003). Sotillos and Campuzano constructed a dominant-negative form of *RacGap50C*, which abolishes the GAP activity while retaining the ability to bind Rac. When expressed in the wing, this construct caused a range of defects, including increased width and fusion of veins, enlarged cells and an increased number of sensory organs, as well as an expansion of the EGF

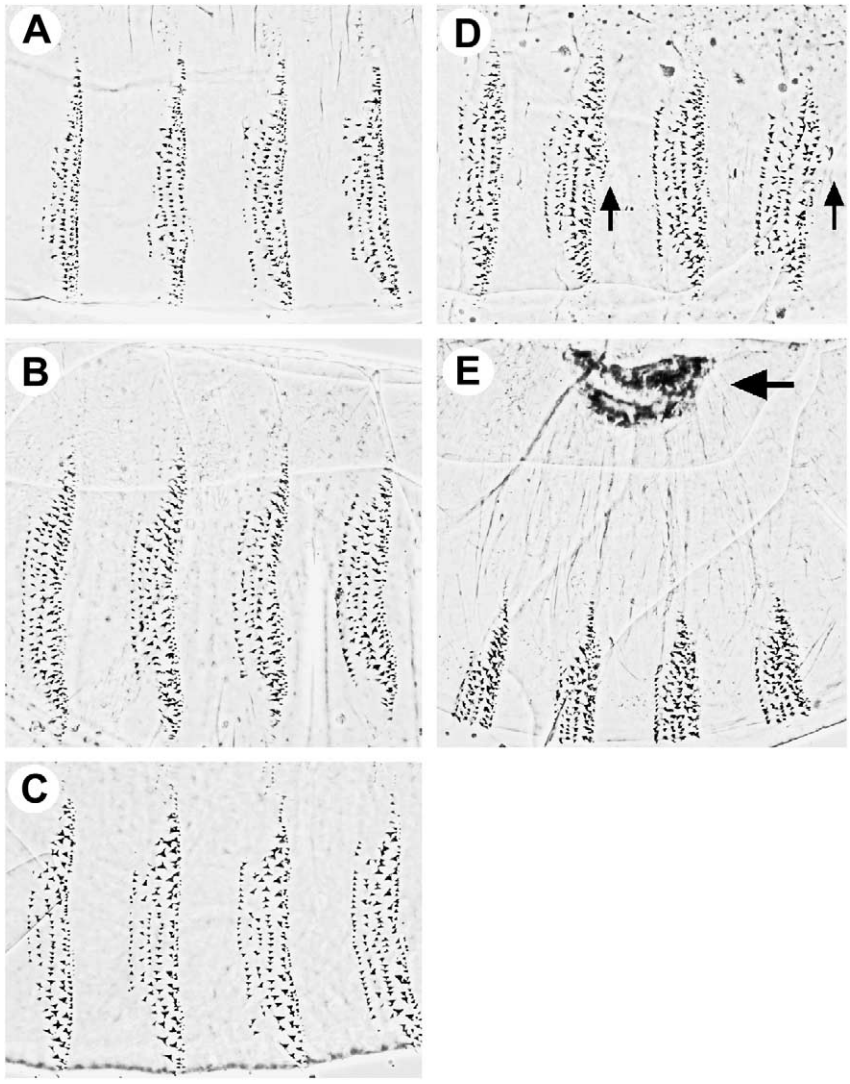


FIGURE 3.—The *AR2* and *DH15* mutant phenotype is rescued by *RacGap50C* expression and is not mimicked by *Rac1* manipulation. The *AR2* homozygous-mutant cuticle pattern defect (A) is substantially rescued by uniformly expressing a *UAS-RacGap50C* transgene with *E22C-Gal4* (B). (C) Rescue is also observed with the *UAS-RacGap50C*$^{\Delta EIE}$ transgene, which carries a small deletion within the GAP domain (SOTILLOS and CAMPUZANO 2000), suggesting that the GTPase-activating function is not required for epidermal patterning. (D) Using *wg-Gal4* to drive expression of the constitutively activated *Rac1* transgene, *UAS-Rac*$^{V12}$, does not mimic the *RacGap50C* phenotype. Instead, it causes excess specification of denticles (arrows), suggesting a loss rather than a gain of Wg pathway activity. (E) Using the *arm-Gal4* driver to uniformly overexpress the dominant-negative *Rac1* transgene, *UAS-Rac*$^{N17}$, does not affect ventral patterning, but causes a dorsal hole phenotype (large arrow) as expected from previous studies (LUO *et al.* 1994).

signaling marker, diphosphoERK, in the presumptive veins (SOTILLOS and CAMPUZANO 2000). These wing phenotypes are enhanced by coexpression of *Rac1*, leading these authors to conclude that Rac1 is a target of RacGap50C activity in the wing. In contrast, Rac1 has been shown to be irrelevant for the cytokinesis role of *RacGap50C*, where the primary function of RacGap50C is to serve as an adaptor molecule linking the microtubule and actin cytoskeletons. This linkage is essential for positioning the contractile ring of dividing cells; expression of a dominant-negative form of *RacGap50C* results in accumulation of multinucleate cells (SOMERS and SAINT 2003). The other Drosophila RacGap, *RacGap84C*, encodes a protein 47% similar to RacGap50C. No point mutations in *RacGap84C* have been identified, but deficiencies in the area are known to cause defects in spermatid and retinal differentiation (BERGERET *et al.* 2001); thus both RacGaps are likely to be functional.

Since mutations in *RacGap50C* were detected in both of our mutant lines, it seemed likely that *RacGap50C* was the gene responsible for the cuticle phenotypes observed. We find that *RacGap50C* mRNA transcripts appear to be maternally contributed to the egg, because early stage embryos show strong staining in RNA *in situ* hybridization experiments (Figure 2B). Low uniform levels of transcript are detected throughout embryogenesis (Figure 2C), showing that it is zygotically expressed during the stages when Wg signaling determines epidermal pattern. We do not detect any segmental modulation of *RacGap50C* expression. To verify that the *RacGap50C* mutations account for the *AR2* and *DH15* mutant phenotypes, we expressed a wild-type *RacGap50C* transgene (SOTILLOS and CAMPUZANO 2000) in mutant embryos and looked for rescue of the mutant phenotype. Driving ubiquitous expression of the *UAS-RacGap50C* transgene during embryogenesis partially rescues the embryonic lethality and completely rescues the pattern defect of *AR2* homozygous-mutant embryos (Figure 3, A and B). Whereas 25% of the progeny from *AR2* heterozygous parents normally fail to hatch ($n = 593$), <10% fail to hatch ($n = 796$) when *UAS-RacGap50C* is uniformly expressed in embryos. However, the homozygous larvae

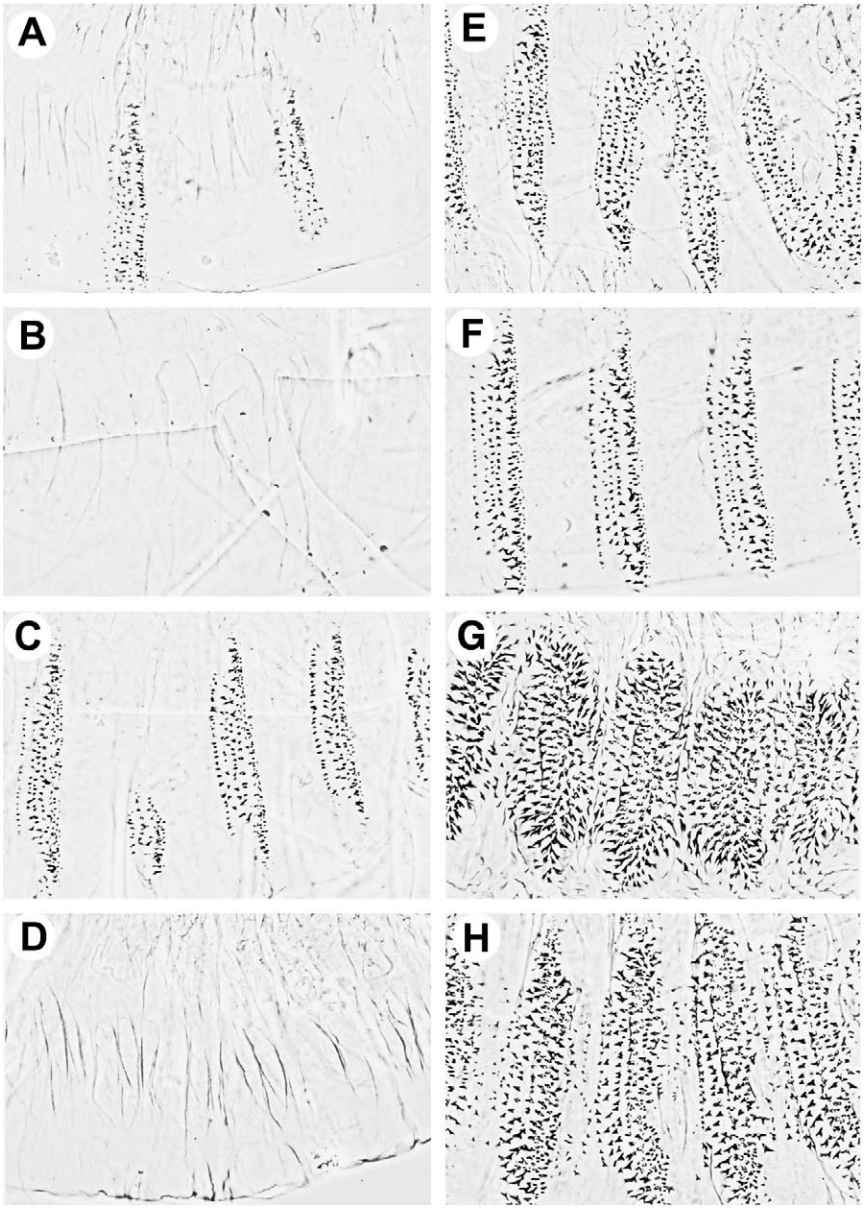


Figure 4.—*RacGap50C* mutations interact genetically with known negative regulators of Wg pathway activity. (A) Embryos homozygous for a strong *nkd* allele, $nkd^{7E89}$, show excessive specification of naked cuticle, but typically retain between one and two denticle belts (see data in Table 1). (B) This phenotype is enhanced in the *AR2;nkd* doubly homozygous embryonic cuticle. (C) The homozygous $nkd^{7E89}$ mutant phenotype is partially suppressed by reducing *wg* dose in the $wg^{CX4}$/+;*nkd/nkd* mutant embryo. (D) This *wg* gene dose effect is lost in the absence of the *RacGap50C* gene product. $wg^{CX4}$ *AR2/+ AR2;nkd/nkd* mutant embryos consistently show the enhanced, uniform naked cuticle phenotype. (E) Driving the *UAS-nkd* transgene uniformly with *E22C-Gal4* causes pattern disruptions in $wg^{CX4}$/+ embryos. (F) This antagonism of Wg pathway activity by *nkd* overexpression is not observed in $wg^{CX4}$ *RacGap50C/++* embryos. (G) Overexpressing a GFP-tagged *UAS-Axin* with *E22C-Gal4* produces severe cuticle pattern defects even in the presence of wild-type levels of Wg signaling. (H) The severity of this Axin-overexpression pattern defect is slightly suppressed in *RacGap50C* homozygous-mutant embryos.

die during larval stages probably because *E22C-Gal4* is expressed only embryonically. Denticle belts of rescued homozygous mutants contain 5.23 ± 0.60 rows of denticles/belt ($n$ = 64), compared to 3.95 ± 0.64 ($n$ = 80) observed in unrescued mutant embryos. These results confirm that the cuticle pattern defect observed in our mutant lines is due to loss of *RacGap50C* function.

***RacGap50C* does not appear to interact with Rac in epidermal patterning:** RacGaps are thought to downregulate activity of Rac by stimulating the intrinsic GTP hydrolysis function of the protein and thereby converting it from the active GTP-bound form to the inactive GDP-bound form (reviewed in Hall 1998). Both the vertebrate and invertebrate RacGTPases are associated with signaling cascades that promote cytoskeletal rearrangements, often during morphological processes. For example, the Drosophila Racs are involved in dorsal closure movements of the embryo, as well as in axon growth and guidance in the developing nervous system (Hakeda-Suzuki *et al.* 2002; Ng *et al.* 2002).

To determine whether the effects of *RacGap50C* in the embryonic epidermis are mediated through a Rho family member, we tested whether the GTPase-activating domain of RacGap50C was required for rescue of the epidermal patterning defect in mutant embryos. The dominant-negative $RacGap50C^{\Delta EIE}$ construct deletes three conserved amino acids in the GAP domain, producing a protein that still binds Rac but cannot stimulate GTP hydrolysis (Sotillos and Campuzano 2000). As mentioned above, Sotillos and Campuzano observed profound effects of this *UAS-*$RacGap50C^{\Delta EIE}$ construct when it is expressed in the wing imaginal disc. In contrast, we find that when we express *UAS-*$RacGap50C^{\Delta EIE}$ ubiquitously in a *RacGap50C* mutant embryo, it is able

**TABLE 1**

**Genetic interactions between *AR2* and *naked***

| Cross | No. of *nkd* mutants | 0 belts | | | 0.5–4 belts | | | 4.5–7.5 belts | | |
|---|---|---|---|---|---|---|---|---|---|---|
| | | Observed | % observed | % expected | Observed | % observed | % expected | Observed | % observed | % expected |
| 1. *nkd/+ × nkd/+* | 124 | 8 | 6 | 0 | 113 | 91 | 100 | 3 | 2 | 0 |
| 2. *AR2/+;nkd/+ × AR2/+;nkd/+* | 265 | 86 | 32 | 25 | 175 | 66 | 75 | 4 | 2 | 0 |
| 3. *wg/+;nkd/+ × nkd/+* | 118 | 8 | 7 | 0 | 53 | 45 | 50 | 57 | 48 | 50 |
| 4. *wg AR2/++;nkd/+ × AR2/+;nkd/+* | 302 | 64 | 21 | 25 | 170 | 56 | 50 | 67 | 22 | 25 |

Only *nkd* homozygous-mutant embryos are categorized; these represented ~25% of the total fertilized eggs laid in each cross. Expected percentages for crosses 2 and 4 are based on our hypothesis that *AR2* homozygosity enhances the severity of the *nkd* mutant phenotype. Expected percentages for cross 3 are based on previous observations that *wg* heterozygosity suppresses the *nkd* mutant phenotype (Bejsovec and Wieschaus 1993). Note that variability in the *nkd* single-mutant phenotype (cross 1) accounts for the divergence between observed and expected frequencies in crosses 2 and 3; when this is taken into consideration, the observed and expected numbers are not significantly different. This does not appear to be true for cross 4, suggesting that reduced *wg* gene dose slightly diminishes the ability of *RacGap50C* mutations to enhance the *nkd* mutant phenotype.

to rescue the cuticle pattern phenotype (Figure 3C). The rescued homozygous-mutant embryos have 4.81 ± 0.60 rows of denticles/belt ($n$ = 160). This rescue is not as complete as that observed for the wild-type *RacGap50C* construct (5.23 ± 0.60 rows of denticles/belt, above) and does not include any rescue of the embryonic lethality as was observed for the wild-type construct. However, the cuticle phenotype is significantly different from the unrescued *RacGap50C* mutant ($P$ = 0.001). Overexpressing the *UAS-RacGap50C$^{\Delta EIE}$* transgene in a wild-type embryo does not produce any detectable patterning defect nor does it appear to affect larval viability (data not shown). These results suggest that *RacGap50C* has a novel function in epidermal patterning that does not involve interaction with a GTPase.

To further confirm that the GTPase-activating function of *RacGap50C* is dispensable for epidermal patterning, we tested the effects of Rac activity in patterning. Since GTPase activation would be expected to turn Rac off, a constitutively active Rac would be expected to produce phenotypes similar to loss of *RacGap50C* in processes where its GAP activity is relevant. We therefore tested whether the patterning defects of our *RacGap50C* mutants could be mimicked by expression of the constitutively activated *Rac1* transgene, *UAS-Rac$^{V12}$* (Luo *et al.* 1994). We used several different embryonic *Gal4* drivers to express the *UAS-Rac$^{V12}$* transgene, but most caused the embryos to die prior to secretion of the cuticle, making it impossible to score cuticle pattern alterations. Expressing *Rac$^{V12}$* in the spatially restricted *wg* domain in each segment, using the *wg-Gal4* driver, does not block cuticle secretion but these embryos produce a cuticle pattern very different from the *RacGap50C* loss-of-function phenotype (Figure 3D). Rather than the expected hyperactivation, the resulting cuticles show defects more consistent with a reduction in Wg signaling, even though Wg protein levels are unaffected (not shown). Furthermore, overexpression of a dominant-negative form of *Rac1*, *UAS-Rac$^{N17}$* (Luo *et al.* 1994), with most embryonic drivers tested does not produce any disruption of ventral epidermal patterning, although dorsal closure is clearly disrupted as previously reported (Figure 3E). We conclude that *RacGap50C* does not act through Rac in promoting its effects on embryonic pattern formation.

***RacGap50C* interacts with negative regulators of the Wg pathway:** The increased specification of naked cuticle in *AR2* and *DH15* mutant embryos suggests an increase in Wg pathway activity similar to that observed in mutants disrupting known negative pathway regulators. Most of these negative regulator mutations have a strong maternal effect, and the excess naked cuticle phenotype is observed only when maternal contribution is reduced (Siegfried *et al.* 1992; Hamada *et al.* 1999; McCartney *et al.* 1999). The exception is *nkd*, which acts zygotically (Jürgens *et al.* 1984) as do the *AR2* and *DH15* mutations. *nkd* encodes a protein that interacts with the Wg pathway at the level of Dsh, to which it binds through the Dsh basic-PDZ region (Zeng *et al.* 2000; Rousset *et al.* 2001). *nkd* mutant embryos show an excess of naked cuticle at the expense of denticle belts, and this phenotype is enhanced by *RacGap50C* mutations. There is some variability in the *nkd* mutant phenotype, but on average *nkd* mutants produce 1.5 abdominal denticle belts (Figure 4A; Table 1), as opposed to the 8 abdominal belts seen in wild type. The denticles formed in the few *nkd* mutant belts are normally patterned, with typical denticle morphologies (Bejsovec and Wieschaus 1993). In contrast, the average phenotype of *RacGap50C*; *nkd* doubly homozygous mutants is uniform naked cuticle, showing no denticle belts at all (Figure 4B; Table 1).

The *nkd* mutant phenotype is sensitive to *wg* gene

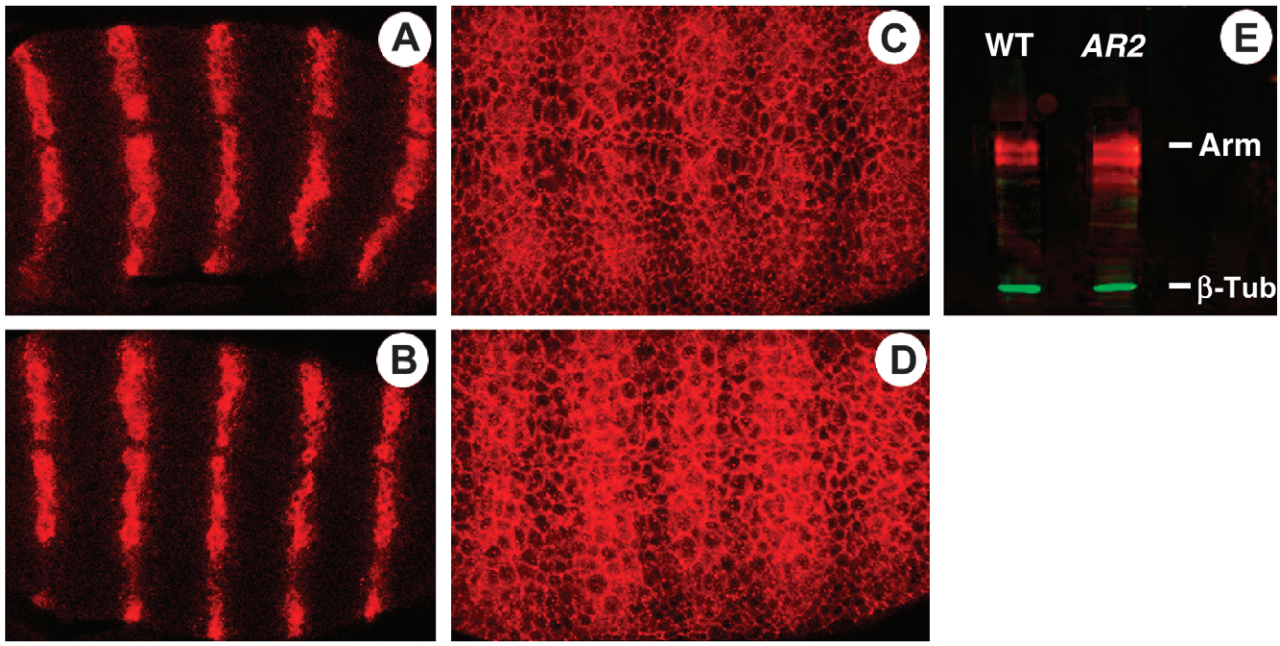


FIGURE 5.—*RacGap50C* mutant embryos have normal Wg levels, but show elevated Arm protein accumulation. (A) Anti-Wg antibody staining in wild-type stage 10 embryos shows segmental stripes, with a slightly punctate appearance due to secretion and endocytosis of the protein. (B) Anti-Wg antibody staining in *RacGap50C* homozygous embryos is indistinguishable from that of wild type. (C) Anti-Arm antibody staining in wild-type stage 10 embryos shows broad stripes of higher accumulation, reflecting the domain of cells responding to the Wg signal in each segment. (D) The segmental striping of Arm is still observed in *RacGap50C* homozygous-mutant embryos, but accumulation of Arm appears to be higher throughout the epidermis. All embryos shown are siblings from the *AR2/Kr-Gal4 UAS-GFP CyO* stock; both antibody reactions were double labelings with the GFP antibody to distinguish homozygous mutants from their *CyO*-bearing heterozygous or homozygous wild-type siblings. Embryo pairs [(A and B) and (C and D)] are from the same slide preparations and confocal images were captured under identical conditions. (E) Immunoblotting lysates of hand-selected embryos confirms the impression that Arm levels are higher in the homozygous mutants. Comparison of Arm levels normalized to the tubulin loading control indicates that Arm levels are 25% higher in the AR2 mutant homozygotes than in their wild-type, *CyO*-bearing siblings.

dosage: heterozygosity for a *wg* null allele partially suppresses the ectopic naked cuticle specification of *nkd* homozygotes (BEJSOVEC and WIESCHAUS 1993). *RacGap50C* mutations remove the ability of lowered Wg dose to suppress the *nkd* mutant phenotype. Embryos homozygous for *nkd* and heterozygous for $wg^{CX4}$ typically show a range of between 4.5 and 7.5 abdominal denticle belts (Figure 4C; Table 1), as opposed to the 1.5 average for *nkd* single mutants. This rescue is reversed when the *AR2* or *DH15* mutation is placed in the background. Embryos homozygous for both *RacGap50C* and *nkd*, and heterozygous for $wg^{CX4}$, secrete uniform naked cuticle with no denticle belts (Figure 4D; Table 1). Thus *RacGap50C* activity is required for the *wg* dose sensitivity of *nkd*.

Since *RacGap50C* mutations are enhancers of the *nkd* loss-of-function phenotype, we wondered how they would behave in *nkd* gain-of-function experiments. Ubiquitous overexpression of *nkd* in a wild-type embryo produces no cuticle pattern defect unless the gene dosage of *wg* is reduced (ZENG *et al.* 2000). In $wg^{CX4}$ heterozygous embryos, overexpressing *nkd* produces fusions between denticle belts due to loss of the intervening naked cuticle (Figure 4E). Thus, when Wg levels are limiting, ectopic Nkd activity can antagonize the pathway. We find that reducing the dose of *RacGap50C* reverses this effect. Embryos heterozygous for $wg^{CX4}$ and *RacGap50C* show a wild-type cuticle pattern when *nkd* is overexpressed (Figure 4F). This series of experiments demonstrates that *RacGap50C* has a synergistic interaction with Nkd, a negative regulator of the Wg pathway, suggesting that *RacGap50C* also is required for negative pathway regulation.

We find similar interactions with Axin, another negative regulator of the Wg pathway. Overexpression of a GFP-tagged *Axin* transgene causes cuticle pattern defects consistent with severely compromised Wg signal transduction. The embryos show a "lawn of denticles" pattern similar to *wg* loss-of-function mutants (Figure 4G). However, when *Axin* is overexpressed in *RacGap50C* mutant embryos, the resulting phenotype is not as severe. Some aspects of the segmental pattern are rescued, with more naked cuticle separating the denticle belts (Figure 4H). Thus loss of *RacGap50C* gene activity can partially suppress Axin overexpression phenotypes, suggesting that the *RacGap50C* mutations disrupt a pathway component that either is a limiting cofactor for Axin or acts downstream of Axin in the Wg signaling pathway.

***RacGap50C* mutations affect Arm accumulation:** To

determine where in the Wg pathway *RacGap50C* acts, we analyzed molecular markers of Wg signaling. The *wg* gene is expressed in a one-cell-wide stripe in each segment of the developing embryo. *wg* itself is a target gene activated by Wg signaling: disruption of various pathway components can alter *wg* gene expression or Wg protein secretion or distribution. However, we find that Wg protein distribution is indistinguishable from wild type in the *RacGap50C* mutant embryos (Figure 5, A and B), indicating that the mutations disrupt neither expression nor protein accumulation. We also examined expression of *engrailed*, another target gene for Wg activity (DiNardo *et al.* 1988; Martinez Arias *et al.* 1988), and found no significant change in its pattern or level compared with wild type (not shown).

In contrast, the levels of Arm protein accumulation are significantly altered in *RacGap50C* mutants compared with wild type. *arm* mRNA is expressed at uniform levels throughout the epidermis (Riggleman *et al.* 1989), but Arm protein accumulates in a striped pattern in wild-type embryos, reflecting the segmental stripes of high Wg signaling activity (Riggleman *et al.* 1990; Peifer *et al.* 1994). In *RacGap50C* mutant embryos, Arm accumulation appears to be elevated compared to wild type (Figure 5, C and D). This increase in Arm protein is confirmed by immunoblot analysis. The *RacGap50C* mutant chromosomes were balanced over a *CyO* chromosome bearing a *Kruppel*-driven *GFP* transgene insert. This allows identification and selection of homozygous-mutant embryos by their failure to fluoresce. At stage 10, homozygous-mutant embryos show between 20 and 25% higher steady-state levels of Arm protein compared to their fluorescing wild-type siblings (Figure 5E). Although these increases are not as extreme as those observed for maternal and zygotic loss of *zw3*, the principal agent of Arm destruction (Peifer *et al.* 1994), they represent the most dramatic zygotic phenotype documented.

**The *RacGap50C* cell cycle defects are unrelated to epidermal patterning defects:** Previously, the Saint lab has shown by RNA interference that *RacGap50C* is required for cytokinesis in cell culture and in imaginal disc tissue (Somers and Saint 2003). This requirement for *RacGap50C* in cell division explains why we have been unable to obtain sizable clones of *RacGap50C* mutant tissue in germline and somatic mosaic experiments (data not shown). This has prevented us from assessing the mutant effects of reducing maternal contribution for the *RacGap50C* gene product. The abundant *RacGap50C* mRNA detected in early stage embryos (Figure 2B) suggests that substantial maternal product is contributed to the egg. This maternal product most likely accounts for the relatively normal cell division that we observe in the *RacGap50C* mutant embryos through most of development. Work on our mutant lines in the Saint laboratory indicates that cell division defects can be detected in late stage embryos, with binucleate cells accumulating in the epidermis during stage 11 (M. Zavortink and R. Saint, personal communication).

The epidermal patterning defects that we observe are not, however, a secondary consequence of late defects in cytokinesis. First, we observe changes in Armadillo stabilization beginning at stage 9, whereas the cell division defects observed by the Saint laboratory do not become apparent until stage 11. Second, we find that the cuticle pattern defect is rescued by ectopic expression of the *UAS-RacGap50C*$^{\Delta EIE}$ transgene (Figure 3C), whereas the cytokinesis defect is not (Somers and Saint 2003). Third, we have found another experimental condition that rescues the epidermal patterning defects of *RacGap50C* homozygotes without rescuing the cytokinesis defects. Antagonizing Wg pathway activity by ectopically overexpressing *nkd* significantly reverses the cuticle pattern defects of *RacGap50C* mutant embryos (Figure 6, A and B), although it does not alter their embryonic lethality. *RacGap50C* homozygous embryos overexpressing *nkd* produce 5.25 ± 0.47 rows of denticles/belt ($n$ = 80), comparable to the measurements obtained for mutant embryos rescued with the wild-type *RacGap50C* transgene. Thus ectopic Nkd activity can partially compensate for loss of the *RacGap50C* activity in Wg-mediated patterning events and allows *RacGap50C* mutant embryos to secrete a pattern more similar to that of the wild-type state (Figure 6C). However, we observe large, binucleate cells accumulating in *nkd*-overexpressing *RacGap50C* mutant embryos at the same frequency as they do in the *RacGap50C* homozygotes alone (Figure 6, D and E), even though epidermal patterning defects are substantially rescued in the *nkd*-overexpressing embryos. Wild-type embryos at the same stage (Figure 6F) do not accumulate binucleate cells and show a higher cell density in the epidermal epithelium than do the *RacGap50C* mutant embryos. Thus the role of *RacGap50C* in Wg pathway modulation is separable from its role in forming the contractile ring during cytokinesis.

## DISCUSSION

Involvement of a Rac GTPase-activating protein homolog in Wg signaling is unexpected and unprecedented and may reveal a novel function that does not involve a Rho family GTPase. We find that *RacGap50C* interacts genetically with *nkd* and appears to act at the same level or downstream of Axin in the control of Arm stabilization. Our data indicate that RacGap50C probably does not act through Rac1 to negatively regulate Wg activity, nor are other GTPases likely to be involved in this aspect of epidermal patterning since the cuticle defects of mutant embryos can be rescued by a form of RacGap50C that lacks catalytic residues in the GTPase-activating domain. Moreover, previous work shows that other Rho family members are unlikely to be involved in Wg-mediated patterning. Overexpressing either constitutively active or dominant-negative *Rho*, *Rac*, or *cdc42* transgenes disrupts dorsal closure but does not appear to affect ventral patterning (Luo *et al.* 1994; Harden *et al.* 1999). Loss of maternal *Rho* activity has

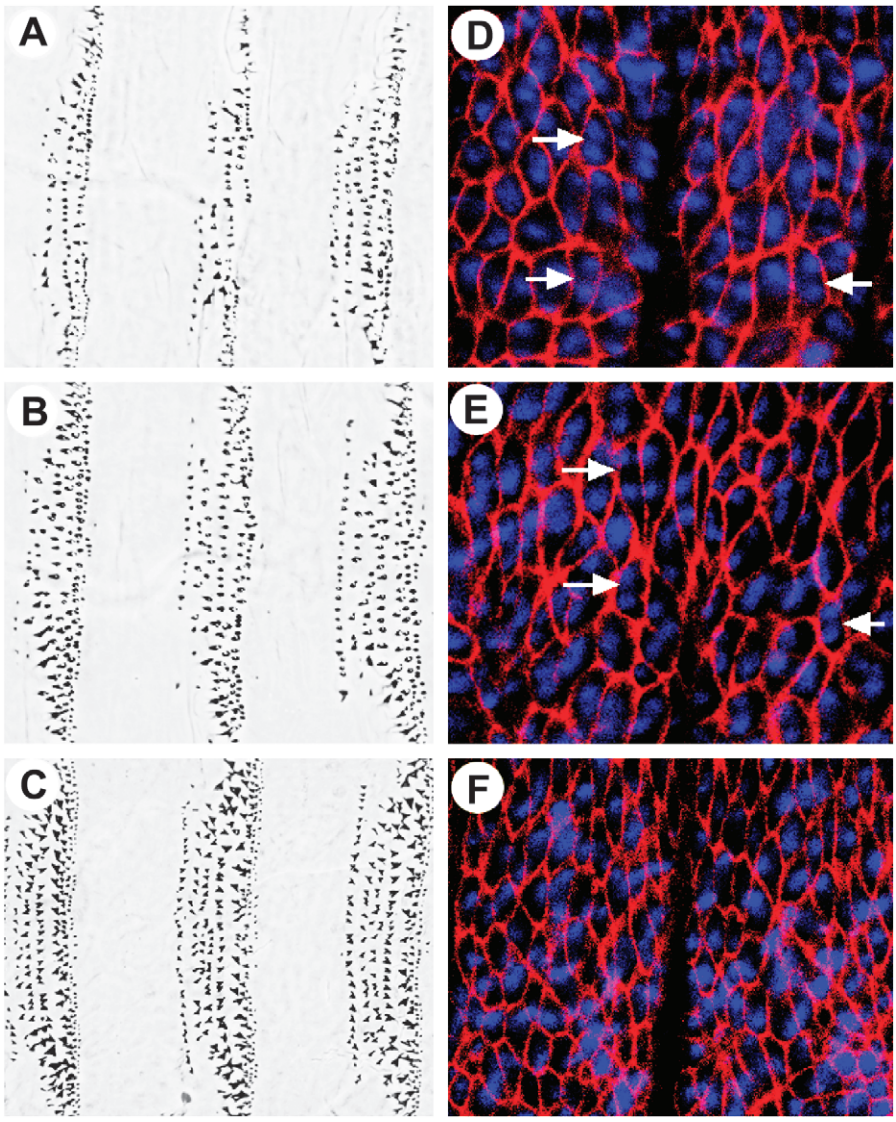


Figure 6.—Naked overexpression rescues the *RacGap50C* cuticle pattern defect without affecting the cytokinesis defect. (A) *AR2* mutants show the characteristic loss of denticles, particularly in the more anterior rows of the denticle belt. (B) Driving the *UAS-nkd* transgene ubiquitously with *E22C-Gal4* significantly rescues the cuticle pattern defect, to a pattern much more closely resembling that of wild type (C). The *UAS-nkd* and the *E22C-Gal4* transgenes were independently recombined onto the *AR2* mutant chromosome, and these lines were then crossed to each other. Therefore all *AR2* homozygotes in this experiment overexpress *nkd*. (D) The *AR2* homozygous-mutant embryos accumulate large, binucleate cells (arrows) during stage 11, visualized with DAPI staining in blue to show nuclei and anti-Coracle staining (Fehon *et al.* 1994) in red to outline the cell membranes. During stage 11, the segmental furrows begin to form; one is shown here and in E and F as a vertical cleft in the field of epidermal cells. (E) The accumulation of binucleate cells is unaffected in *AR2* mutant homozygotes that are overexpressing *nkd*. Thus the *RacGap50C* cytokinesis defects are unrelated to the epidermal patterning defects, which are rescued by this treatment (B). (F) The epidermal cell density is higher in stage 11 embryos that have wild-type cytokinesis. No binucleate cells are apparent in the wild-type, *CyO*-bearing siblings nor in Oregon-R embryos of the same stage, shown here.

been found to alter embryonic segmental pattern, but this is due to an early effect on establishing segmentation gene expression patterns (Magie *et al.* 1999). Ras activation through the EGF signaling cascade has been found to affect epidermal patterning, but in a way that counteracts Wg signaling (O'Keefe *et al.* 1997; Szuts *et al.* 1997). Thus a GTPase-activating protein would be expected to positively influence Wg-mediated patterning if it acted through Ras, rather than the negative influence we observe for *RacGap50C*.

For these reasons, we believe that the role of *RacGap50C* in Wg signaling may instead parallel its role in cytokinesis, where it seems to function primarily as an adaptor molecule. *RacGap50C* was identified by the Saint laboratory through a yeast two-hybrid screen for molecules that interact with *pebble*, a RhoGEF that is essential for cytokinesis (Somers and Saint 2003). Subsequently, they showed that RacGap50C protein also binds to Pavarotti, a kinesin-like molecule, thus forming a bridge between the microtubule and actin cytoskeletons. This adaptor function appears critical for the proper positioning of the acto-myosin contractile ring at the end of mitosis (Somers and Saint 2003).

One could imagine that a structural role for RacGap50C in linking the microtubule and actin cytoskeletons might be relevant to its regulation of Wg pathway activity. Apc2, a scaffolding molecule that is an essential component of the destruction complex, is known to interact with both microtubules and the cortical actin cytoskeleton (McCartney *et al.* 1999, 2001). Mutations that disrupt the cortical localization of Apc2 compromise function of the destruction complex (McCartney *et al.* 1999; A. Bejsovec, unpublished results), suggesting that subcellular localization of the complex may be critical. Furthermore, recent work from the Bienz and Wieschaus laboratories demonstrates that Axin, another scaffolding component in the complex, changes its subcellular localization in response to Wg signaling (Cliffe *et al.* 2003) and is consequently degraded (Tolwinski *et al.* 2003). Thus the positioning of the destruc-

tion complex and/or some of its subunits may play a critical role in regulating its Arm-degrading activity. RacGap50C may be involved directly in linking the destruction complex to the cell cortex to promote its proper activity or may restrict movement of Axin to the cortex for its Wg-mediated destruction. In either case, loss of *RacGap50C* function would reduce the normal degradation of Arm and thereby cause ectopic Wg pathway activity.

Another possible explanation for RacGap50C's effects on Wg pathway activity would not require direct interaction with any pathway component. Rather, some coordination between the microtubule and actin cytoskeletons may be generally required for many different cellular processes. The loss of this adaptor molecule would "loosen" the connection between these two filamentous networks and compromise many cellular events indirectly. It may be that cytokinesis and Wg signal transduction are particularly sensitive to such perturbations or that they simply produce the earliest or most easily detected phenotypes in response to them. A general requirement for microtubule and actin network coordination in destruction complex function could be of great importance in understanding oncogenic Wnt pathway activity. Current work in the laboratory focuses on distinguishing whether RacGap50C interacts specifically with the destruction complex or acts more generally by controlling cellular architecture.

We thank E. Wieschaus, R. Selinger, R. Leung, R. Hays, and H. Dierick for their contributions to early phases of this work; T. Addy for technical assistance; and A. Chao and other members of the Bejsovec laboratory for insightful discussions and comments on the manuscript. We are grateful to the Fehon laboratory for their cheerful help and advice, as well as their generosity with reagents and equipment. We also thank Robert Saint and Michael Zavortink for helpful suggestions and for communicating information before publication. As always we are deeply indebted to the dedicated staff at the Bloomington Stock Center and FlyBase. This work was supported by National Institutes of Health grant GM59068 to A.B.

## LITERATURE CITED

Adams, M. D., S. E. Celniker, R. E. Holt, C. A. Evans, J. D. Gocayne *et al.*, 2000 The genome sequence of *Drosophila melanogaster*. Science **287:** 2185–2195.

Ashburner, M., 1989 *Drosophila: A Laboratory Manual*. Cold Spring Harbor Laboratory Press, Cold Spring Harbor, NY.

Bejsovec, A., and A. Martinez-Arias, 1991 Roles of *wingless* in patterning the larval epidermis of *Drosophila*. Development **113:** 471–485.

Bejsovec, A., and E. Wieschaus, 1993 Segment polarity gene interactions modulate epidermal patterning in *Drosophila* embryos. Development **119:** 501–517.

Bejsovec, A., and E. Wieschaus, 1995 Signaling activities of the Drosophila *wingless* gene are separately mutable and appear to be transduced at the cell surface. Genetics **139:** 309–320.

Bergeret, E., I. Pignot-Paintrand, A. Guichard, K. Raymond, M. O. Fauvarque *et al.*, 2001 RotundRacGAP functions with Ras during spermatogenesis and retinal differentiation in Drosophila melanogaster. Mol. Cell. Biol. **21:** 6280–6291.

Bernards, A., 2003 GAPs galore! A survey of putative Ras superfamily GTPase activating proteins in man and Drosophila. Biochim. Biophys. Acta **1603:** 47–82.

Brunner, E., O. Peter, L. Schweizer and K. Basler, 1997 *pangolin* encodes a Lef-1 homolog that acts downstream of Armadillo to transduce the Wingless signal. Nature **385:** 829–833.

Cadigan, K. M., and R. Nusse, 1997 Wnt signaling: a common theme in animal development. Genes Dev. **11:** 3286–3305.

Chao, A. T., H. A. Dierick, T. M. Addy and A. Bejsovec, 2003 Mutations in eukaryotic release factors 1 and 3 act as general nonsense suppressors in Drosophila. Genetics **165:** 601–612.

Chen, B., T. Chu, E. Harms, J. P. Gergen and S. Strickland, 1998 Mapping of Drosophila mutations using site-specific male recombination. Genetics **149:** 157–163.

Cliffe, A., F. Hamada and M. Bienz, 2003 A role of Dishevelled in recruiting Axin to the plasma membrane during Wingless signaling. Curr. Biol. **13:** 960–966.

Dierick, H. A., and A. Bejsovec, 1998 Functional analysis of Wingless reveals a link between intercellular ligand transport and dorsal-cell-specific signaling. Development **125:** 4729–4738.

Dierick, H., and A. Bejsovec, 1999 Cellular mechanisms of Wingless/Wnt signaling activity. Curr. Top. Dev. Biol. **43:** 153–190.

DiNardo, S., E. Sher, J. Heemskerk-Jongens, J. A. Kassis and P. O'Farrell, 1988 Two-tiered regulation of spatially patterned *engrailed* gene expression during *Drosophila* embryogenesis. Nature **322:** 604–609.

Fehon, R. G., I. A. Dawson and S. Artavanis-Tsakonas, 1994 A *Drosophila* homolog of membrane-skeleton protein 4.1 is associated with septate junctions and is encoded by the *coracle* gene. Development **120:** 545–557.

Hakeda-Suzuki, S., J. Ng, J. Tzu, G. Dietzl, Y. Sun *et al.*, 2002 Rac function and regulation during Drosophila development. Nature **416:** 438–442.

Hall, A., 1998 Rho GTPases and the actin cytoskeleton. Science **279:** 509–514.

Hamada, F., Y. Tomoyasu, Y. Takatsu, M. Nakamura, S. Nagai *et al.*, 1999 Negative regulation of Wingless signaling by D-axin, a *Drosophila* homolog of axin. Science **283:** 1739–1742.

Harden, N., M. Ricos, Y. M. Ong, W. Chia and L. Lim, 1999 Participation of small GTPases in dorsal closure of the *Drosophila* embryo: distinct roles for Rho subfamily members in epithelial morphogenesis. J. Cell Sci. **112:** 273–284.

Jones, W. M., and A. Bejsovec, 2003 Wingless signaling: an axin to grind. Curr. Biol. **13:** R479–R481.

Jürgens, G., E. Wieschaus, C. Nüsslein-Volhard and H. Kluding, 1984 Mutations affecting the pattern of the larval cuticle in *Drosophila melanogaster*. II. Zygotic loci on the third chromosome. Roux's Arch. Dev. Biol. **193:** 283–295.

Logan, C. Y., and R. Nusse, 2004 The Wnt signaling pathway in development and disease. Annu. Rev. Cell Dev. Biol. **20:** 781–810.

Lohs-Schardin, M., C. Cremer and C. Nüsslein-Volhard, 1979 A fate map for the larval epidermis of *Drosophila melanogaster*: localized cuticle defects following irradiation of the blastoderm with a UV laser microbeam. Dev. Biol. **73:** 239–255.

Luo, L., Y. J. Liao, L. Y. Jan and Y. N. Jan, 1994 Distinct morphogenetic functions of similar small GTPases: Drosophila Drac1 is involved in axonal outgrowth and myoblast fusion. Genes Dev. **8:** 1787–1802.

Magie, C. R., M. R. Meyer, M. S. Gorsuch and S. M. Parkhurst, 1999 Mutations in the Rho1 small GTPase disrupt morphogenesis and segmentation during early Drosophila development. Development **126:** 5353–5364.

Martinez Arias, A., N. Baker and P. Ingham, 1988 Role of the segment polarity genes in the definition and maintenance of cell states in the *Drosophila* embryo. Development **103:** 157–170.

McCartney, B. M., H. A. Dierick, C. Kirkpatrick, M. M. Moline, A. Baas *et al.*, 1999 *Drosophila* APC2 is a cytoskeletally-associated protein that regulates Wingless signaling in the embryonic epidermis. J. Cell Biol. **146:** 1303–1318.

McCartney, B. M., D. G. McEwen, E. Grevengoed, P. Maddox, A. Bejsovec *et al.*, 2001 *Drosophila* APC2 and Armadillo participate in tethering mitotic spindles to cortical actin. Nat. Cell Biol. **3:** 933–938.

Moline, M. M., C. Southern and A. Bejsovec, 1999 Directionality of Wingless protein transport influences epidermal patterning in the *Drosophila* embryo. Development **126:** 4375–4384.

Moline, M. M., H. A. Dierick, C. Southern and A. Bejsovec, 2000 Non-equivalent roles of *Drosophila* Frizzled and Frizzled2 in embryonic Wingless signal transduction. Curr. Biol. **10:** 1127–1130.

Ng, J., T. Nardine, M. Harms, J. Tzu, A. Goldstein *et al.*, 2002 Rac GTPases control axon growth, guidance and branching. Nature **416:** 442–447.

Noordermeer, J., P. Johnston, F. Rijsewijk, R. Nusse and P. A. Lawrence, 1992 The consequences of ubiquitous expression of the *wingless* gene in the *Drosophila* embryo. Development **116:** 711–719.

Nüsslein-Volhard, C., E. Wieschaus and H. Kluding, 1984 Mutations affecting the pattern of the larval cuticle in *Drosophila melanogaster:* I. Zygotic loci on the second chromosome. Roux's Arch. Dev. Biol. **193:** 267–282.

O'Keefe, L., S. T. Dougan, L. Gabay, E. Raz, B.-Z. Shilo *et al.*, 1997 Spitz and Wingless, emanating from distinct borders, cooperate to establish cell fate across the Engrailed domain in the *Drosophila* epidermis. Development **124:** 4837–4845.

Peifer, M., and P. Polakis, 2000 Wnt signaling in oncogenesis and embryogenesis—a look outside the nucleus. Science **287:** 1606–1609.

Peifer, M., D. Sweeton, M. Casey and E. Wieschaus, 1994 *wingless* signal and Zeste-white 3 kinase trigger opposing changes in the intracellular distribution of Armadillo. Development **120:** 369–380.

Riggleman, B., E. Wieschaus and P. Schedl, 1989 Molecular analysis of the *armadillo* locus: uniformly distributed transcripts and a protein with novel internal repeats are associated with a *Drosophila* segment polarity gene. Genes Dev. **3:** 96–113.

Riggleman, B., P. Schedl and E. Wieschaus, 1990 Spatial expression of the *Drosophila* segment polarity gene *armadillo* is posttranscriptionally regulated by *wingless.* Cell **63:** 549–560.

Rousset, R., J. Mack, K. Wharton, J. Axelrod, K. Cadigan *et al.*, 2001 *naked cuticle* targets *dishevelled* to antagonize Wnt signal transduction. Genes Dev. **15:** 658–671.

Siegfried, E., T. Chou and N. Perrimon, 1992 *wingless* signaling acts through *zeste-white 3*, the *Drosophila* homolog of *glycogen synthase kinase-3*, to regulate *engrailed* and establish cell fate. Cell **71:** 1167–1179.

Somers, W. G., and R. Saint, 2003 A RhoGEF and Rho family GTPase-activating protein complex links the contractile ring to cortical microtubules at the onset of cytokinesis. Dev. Cell **4:** 29–39.

Sotillos, S., and S. Campuzano, 2000 *DRacGap*, a novel *Drosophila* gene inhibits EGFR/Ras signalling in the developing imaginal wing disc. Development **127:** 5427–5438.

Szuts, D., M. Freeman and M. Bienz, 1997 Antagonism between EGFR and Wingless signalling in the larval cuticle of Drosophila. Development **124:** 3209–3219.

Tautz, D., and C. Pfeifle, 1989 A non-radioactive *in situ* hybridization method for the localization of specific RNAs in *Drosophila* embryos reveals translational control of the segmentation gene *hunchback.* Chromosoma **98:** 81–85.

Tolwinski, N. S., M. Wehrli, A. Rives, N. Erdeniz, S. DiNardo *et al.*, 2003 Wg/Wnt signal can be transmitted through Arrow/LRP5,6 and Axin independently of Zw3/Gsk3 activity. Dev. Cell **4:** 407–418.

van de Wetering, M., R. Cavallo, D. Dooijes, M. van Beest, J. van Es *et al.*, 1997 Armadillo co-activates transcription driven by the product of the *Drosophila* segment polarity gene *dTCF.* Cell **88:** 789–799.

Wieschaus, E., and C. Nüsslein-Volhard, 1986 Looking at embryos, pp. 199–227 in *Drosophila: A Practical Approach*, edited by D. B. Roberts. IRL Press, Oxford.

Wodarz, A., and R. Nusse, 1998 Mechanisms of Wnt signaling in development. Annu. Rev. Cell Dev. Biol. **14:** 59–88.

Zeng, W., K. A. J. Wharton, J. A. Mack, K. Wang, M. Gadbaw *et al.*, 2000 *naked cuticle* encodes an inducible antagonist of Wnt signalling. Nature **402:** 789–795.

Communicating editor: T. C. Kaufman